

Blood-vessels' lumen geometric modeling and quantification in 3D images

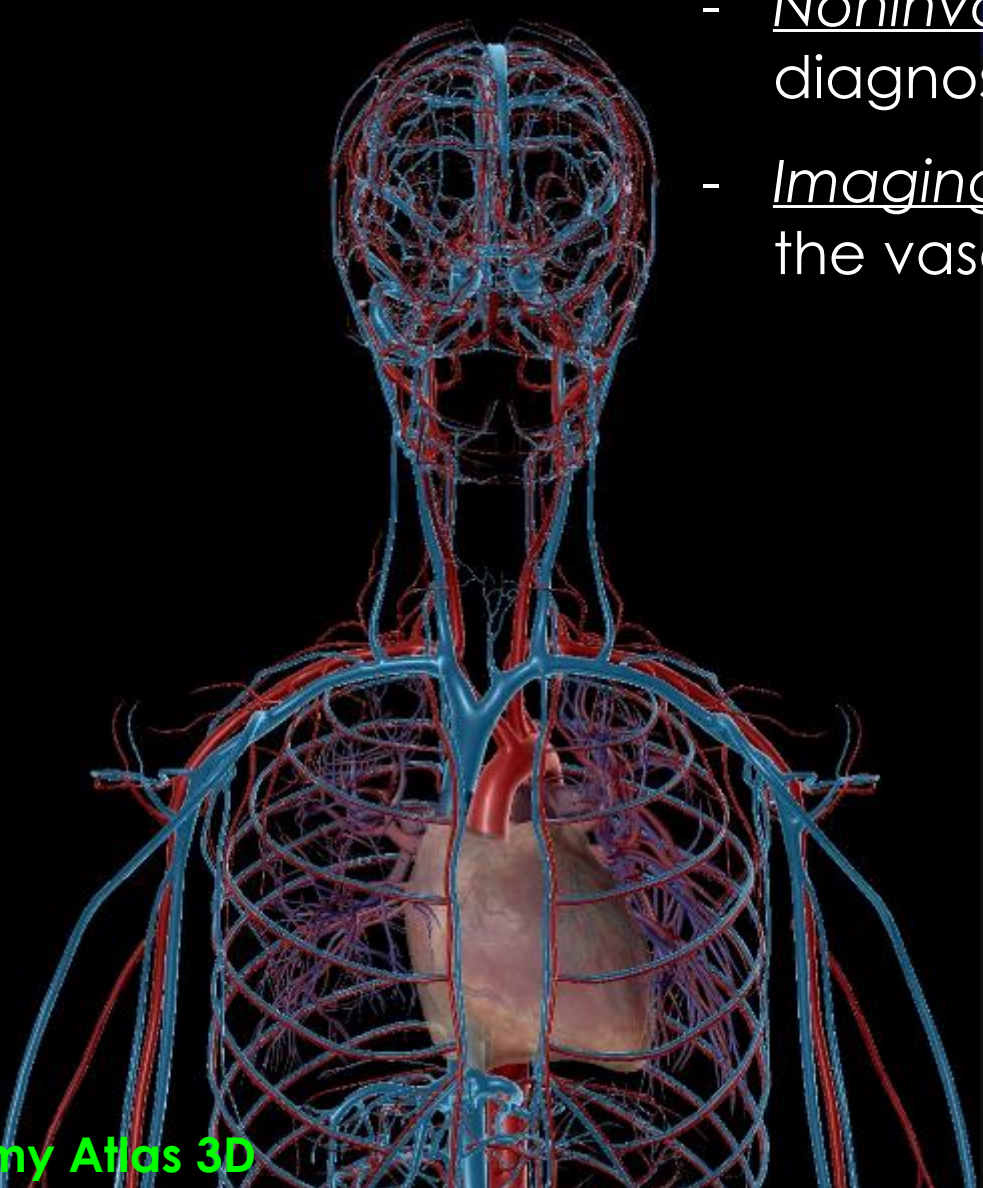
Andrzej Materka and Jakub Jurek
Politechnika Łódzka, Instytut Elektroniki
materka.p.lodz.pl/dydaktyka.html

Overview

- Introduction
- Problem to solve
- Challenges
- Methods
- Examples
- Summary

Introduction

- Cardiovascular diseases are the leading cause of death worldwide [1].
 - They originate mainly from blocked or excessive blood supply to tissues.
-
- Noninvasive, objective and accurate diagnostic techniques are searched for.
 - Imaging techniques play a major role in the vascularity evaluation.



Introduction



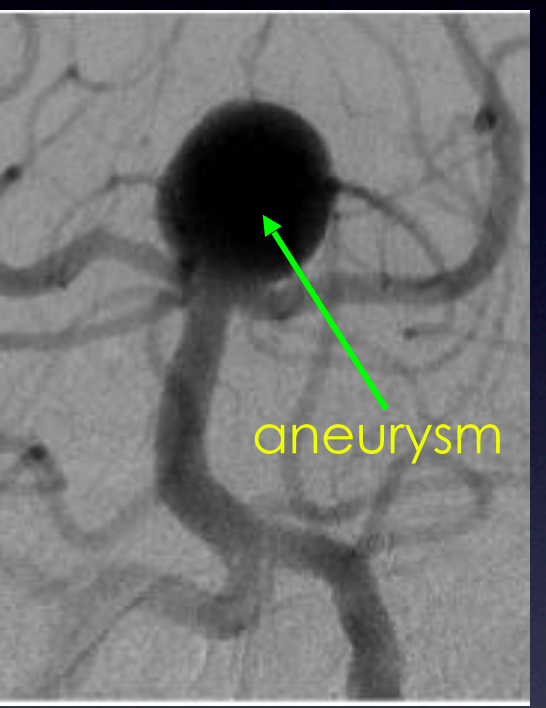
Computed tomography angiography
(CTA)



Magnetic resonance angiography
(MRA)

Personalized quantification of

- lumen centerline course,
- cross-section shape,
- deformations:



Medical imaging

Problem to solve

Lumen geometry reconstruction
of blood vessel trees
given their 3D discrete image

Geometric model

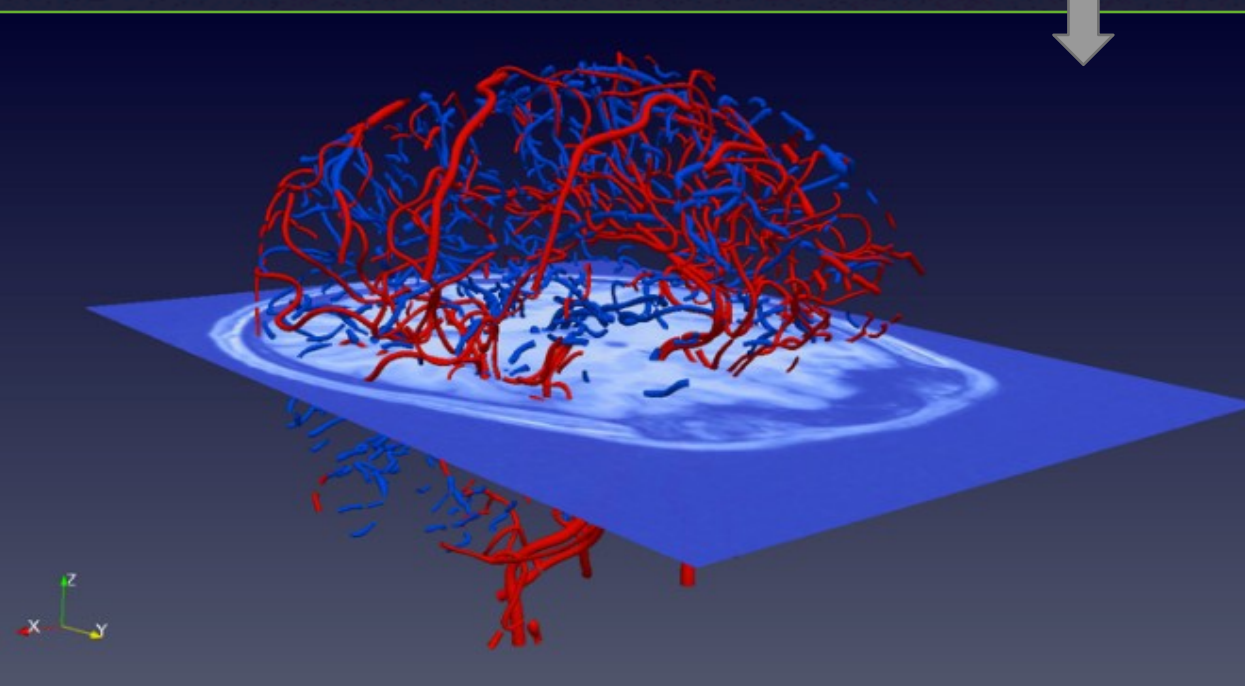
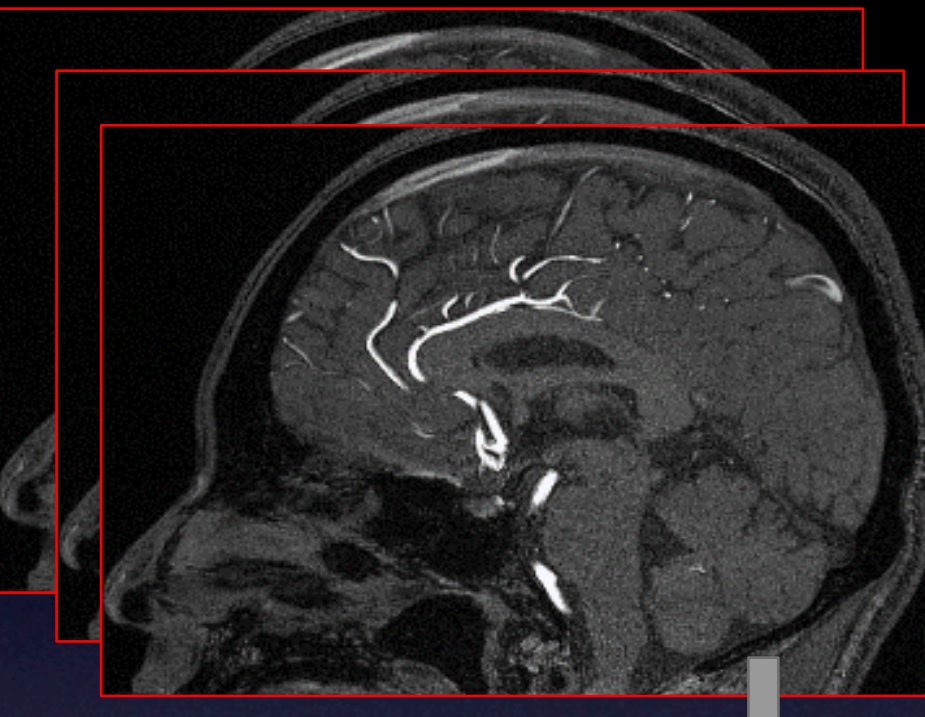
- curved tubes (between n-furcations)
- circular/non-circular cross-sections,
- the diameter varies along the centerline

Basis for

- diagnostic quantification,
- blood-flow simulation,
- surgery planning/execution,
- education, ...

Example

Human brain arteries in ToF MRI

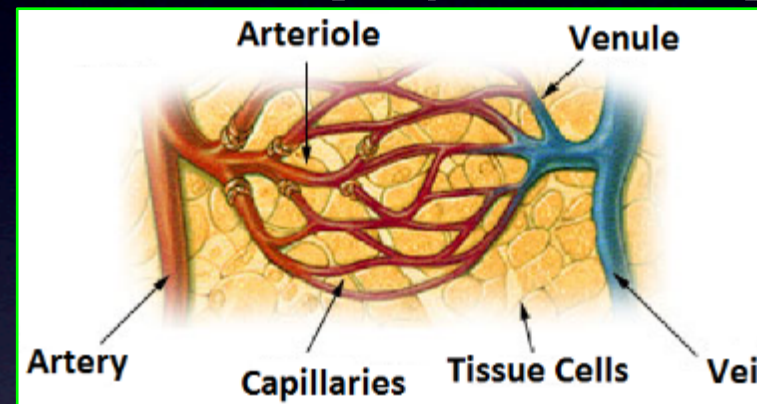


Challenges

The scales

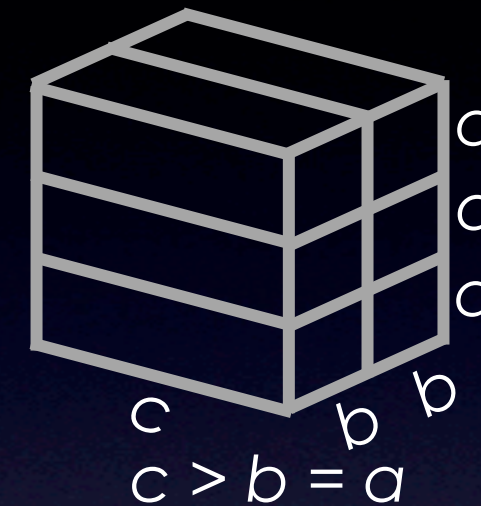
$$\min\{a,b\} \approx 300 \mu\text{m}$$

$$D \in [10 \mu\text{m}, 40 \text{ mm}]$$



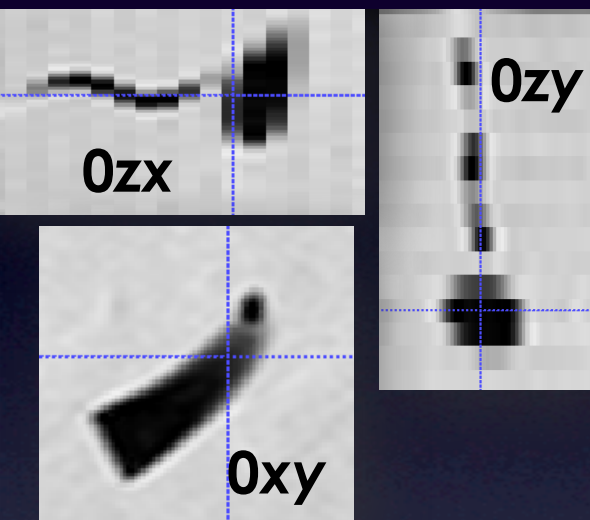
Nieznany autor, licencja: [CC BY-NC](#)

Discretization, voxel anisotropy

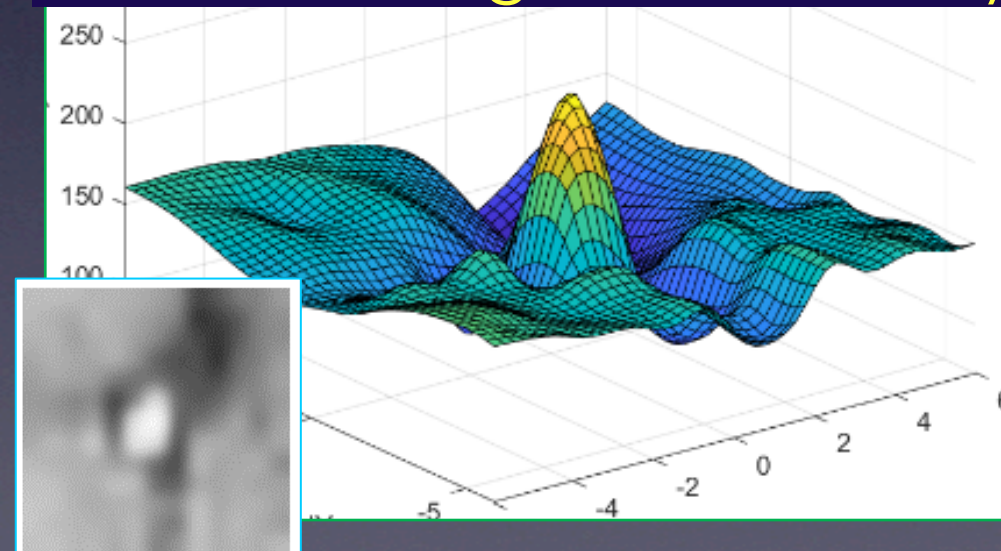


T2w MRI, coronal thick-plane

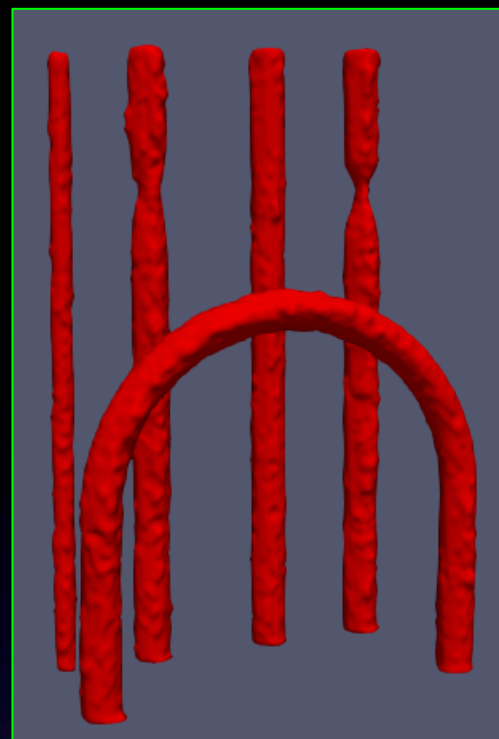
$$0.33\text{mm} \times 0.33\text{mm} \times 2.2\text{mm}$$



Uneven background intensity



Noise (SNR)



Modeling of vascular structures in 3D images

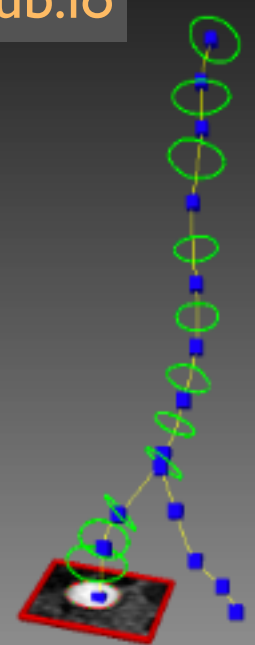
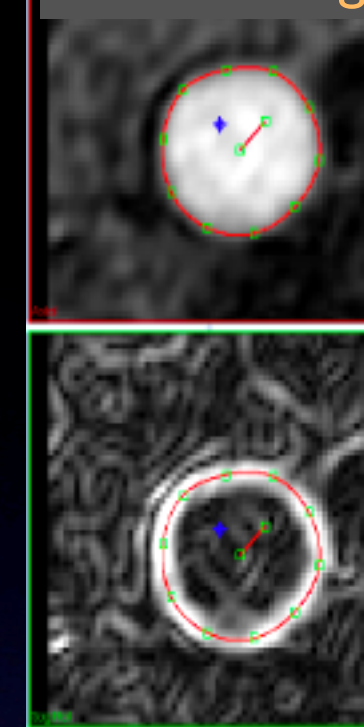
Two main approaches [2,3,5,6]

3D lumen binary segmentation

2D cross-section analysis along approximated centerline

- ✗ loss of information due to binarization [9]
- ✗ voxelized surface needs further smoothing

- ✓ no intermediate binary segmentation
- ✓ incorporation of *a priori* knowledge, for robustness [2]



Methods and algorithms

Level-set techniques [7]

- ✗ long-lasting computations

CNNs [8]

- ✗ need for annotated data

Image model fitting [9,17]

- ✓ subpixel accuracy
- ✗ computationally demanding, local minima

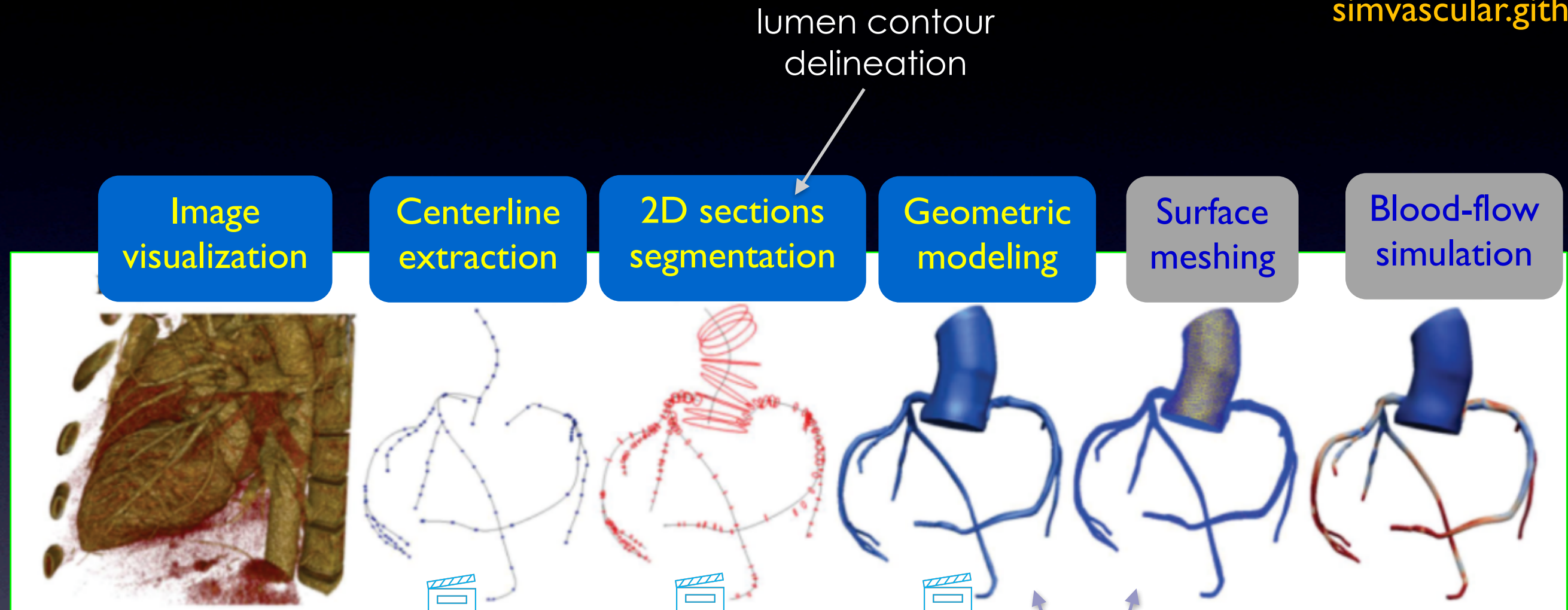
CNN-based parameter estimation [21]

- ✓ subpixel accuracy
- ✓ robustness to background elements
- ✓ very short recall time
- ✓ can be trained on synthetic images

Centerline-based interactive pipeline [22]



simvascular.github.io/



↑
. DICOM
. NIfTI
. ...

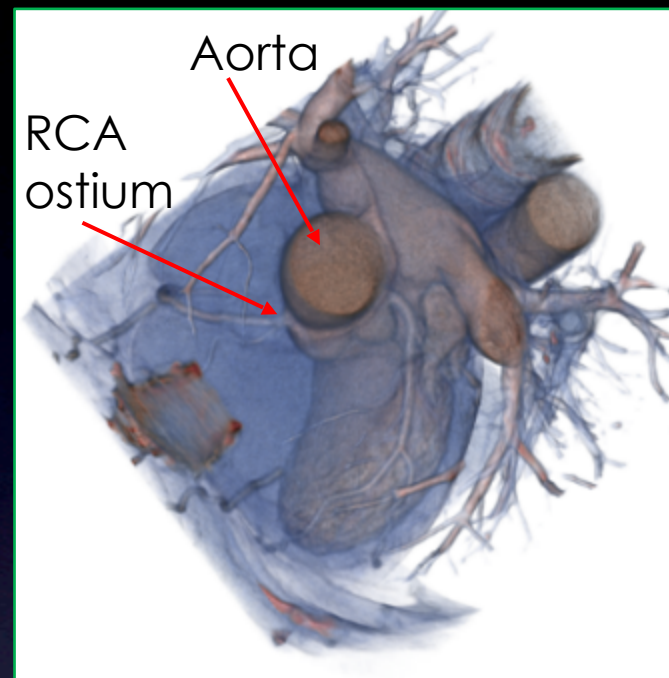
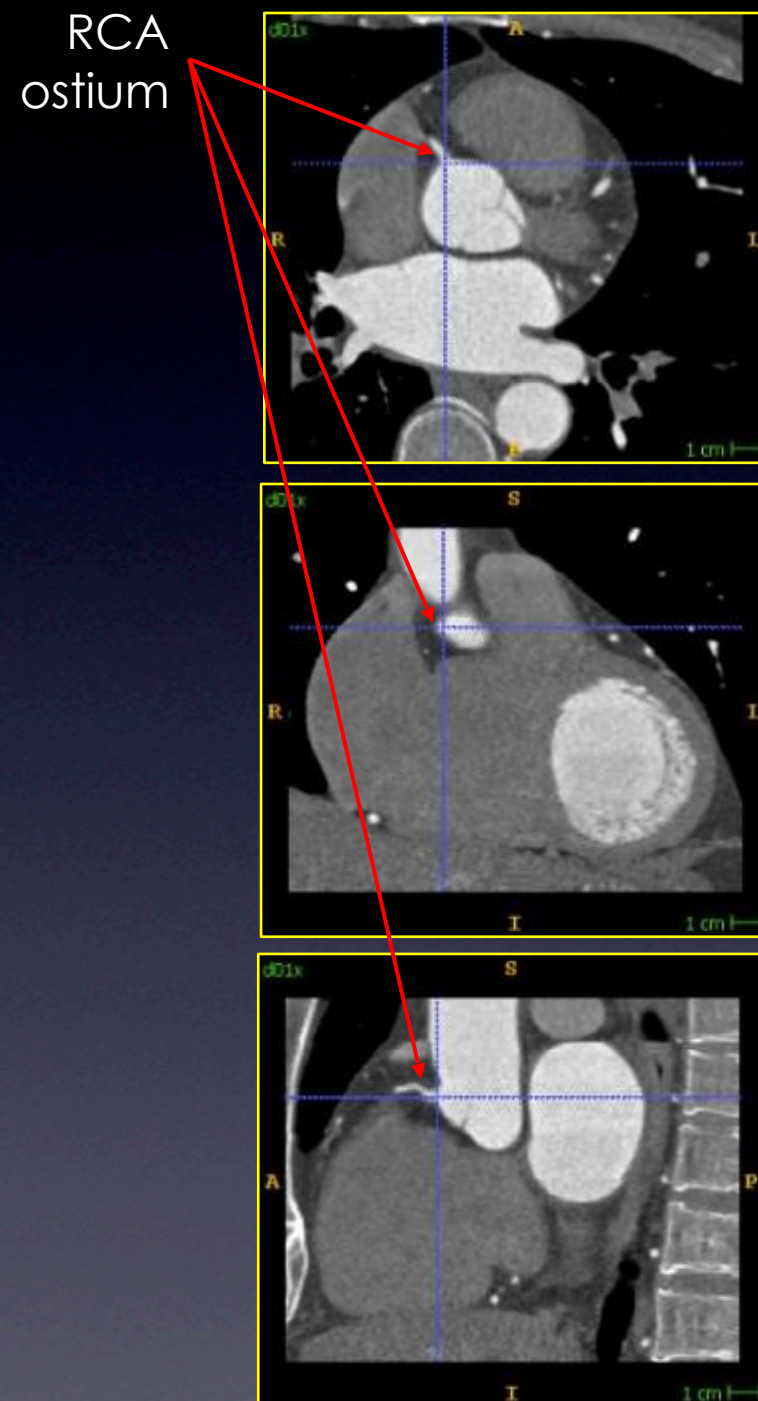
<https://www.pre-scient.com/knowledge-center/geometric-modelling/geometric-modeling.html>

https://community.cadence.com/cadence_blogs_8/b/cfd/posts/hurdling-geometry-model-challenges-for-cfd-mesh-generation

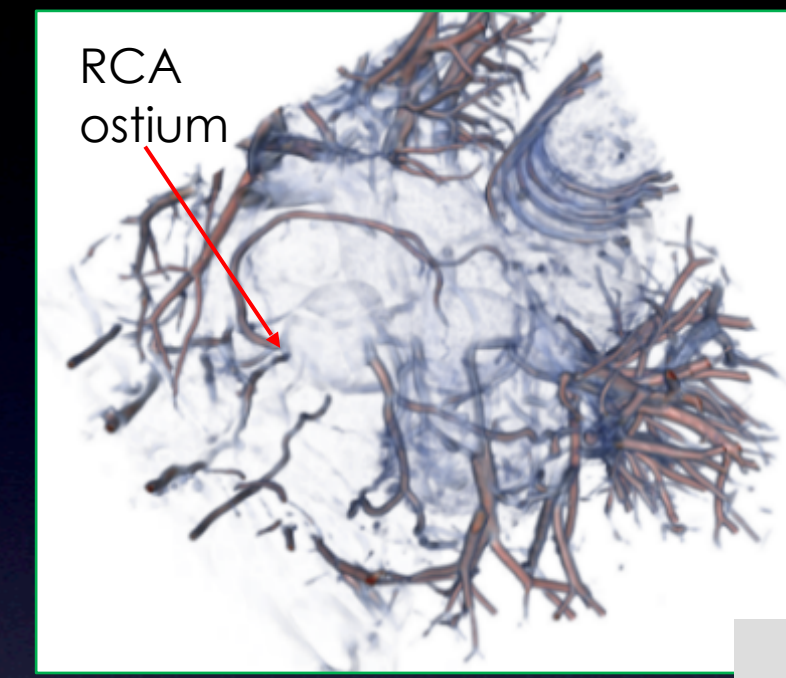
Centerline-based automated pipeline [9,21]

Coronary arteries

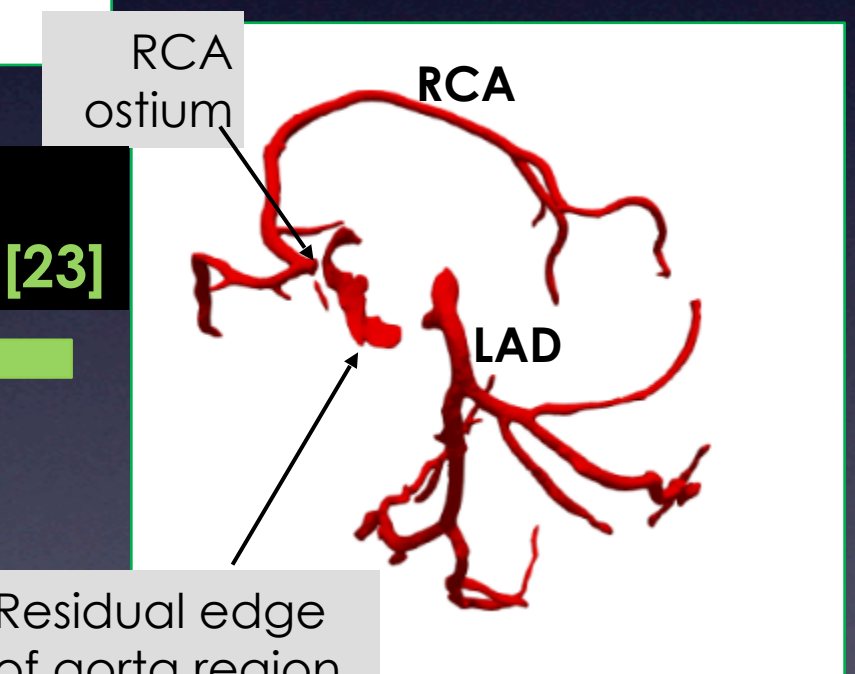
Contrast-enhanced CT [4]



Vesselness filtering
[10,15,16]

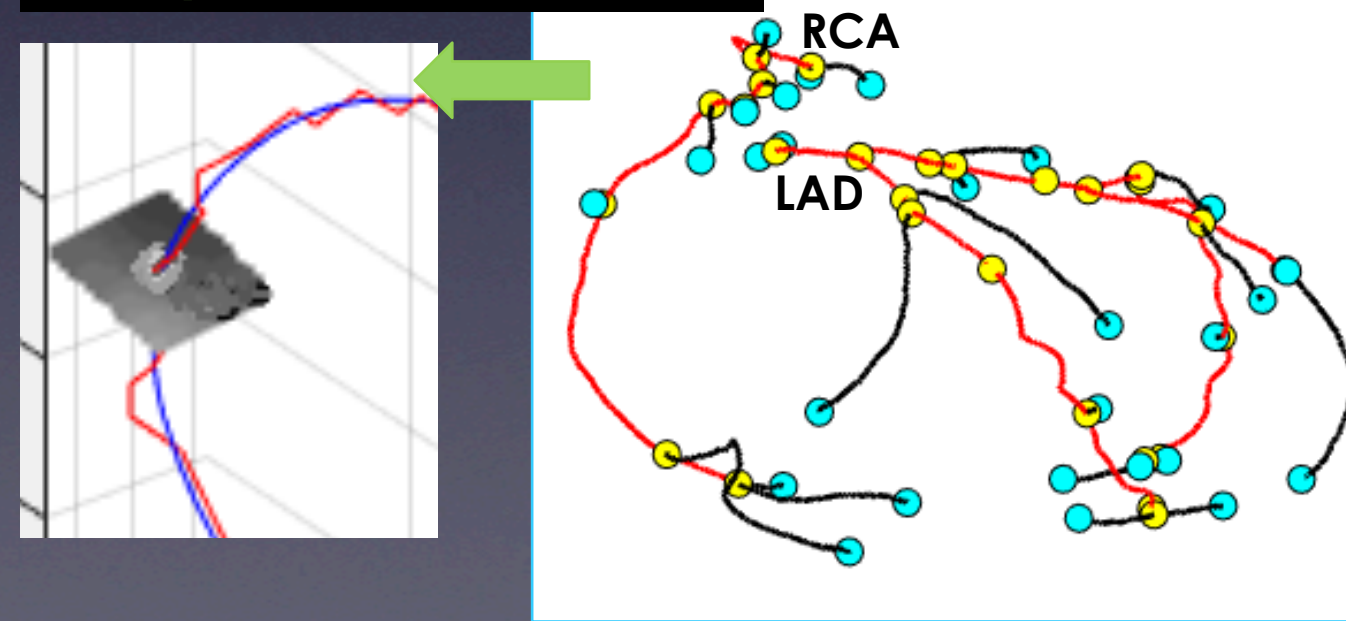


3D region-growing



3D image resampling on cross-section planes

Smooth approximation of binary skeleton branches



RCA - right coronary artery
LAD - left anterior descending

Methods

Image formation model [9,21]

- Scanner assumed to be a linear space-invariant system

$$F(x, y) = \int_{-\infty}^{\infty} \int_{-\infty}^{\infty} f(u, v) h(x - u, y - v) dv du \quad (1)$$

where $f(x,y; a,b,R,d_x,d_y)$ is the lumen intensity distribution
 $h(x,y; w)$ is an isotropic Gaussian impulse response.

Model parameters

a : background intensity

b : intensity step

R : lumen radius

w : 2D Gaussian blur

d_x, d_y : centerline shift

- 2D cross-section intensity at a point (i, j)

$$I(i, j; \theta; \sigma) = a + bF(R, w, i\Delta_s - d_x, j\Delta_s - d_y) + \epsilon(\sigma) \quad (2)$$

where Δ_s is the sampling interval.

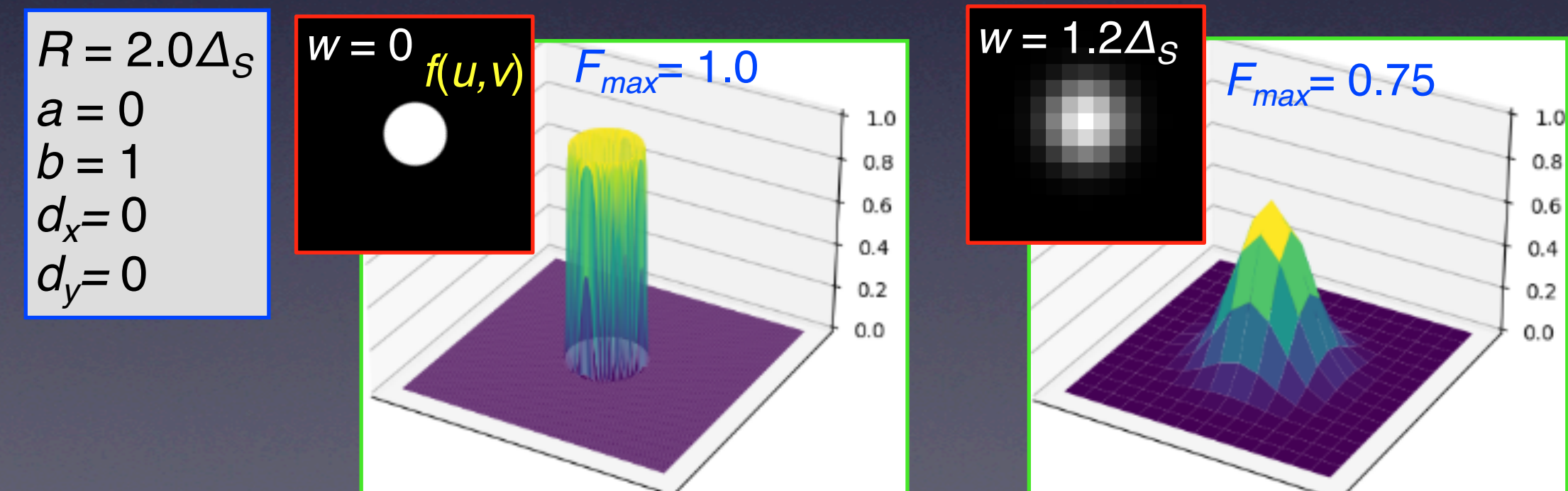
Random noise ϵ

- zero mean

- standard deviation σ

Parameter vector

$\theta = (a, b, R, w, d_x, d_y)$



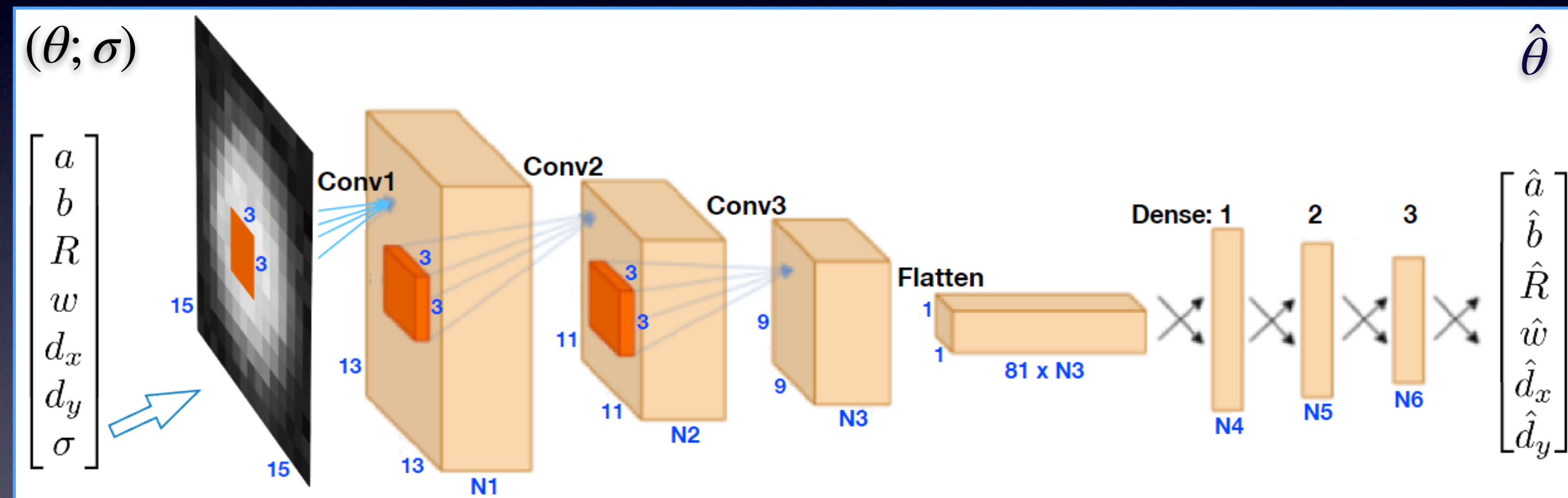
CNN-based lumen parameters estimation [21,13]

Transfer learning

A set of 2D images is computed

$$I_m = I(m, \theta_m, \sigma), \quad m \in \{1, \dots, M\}$$

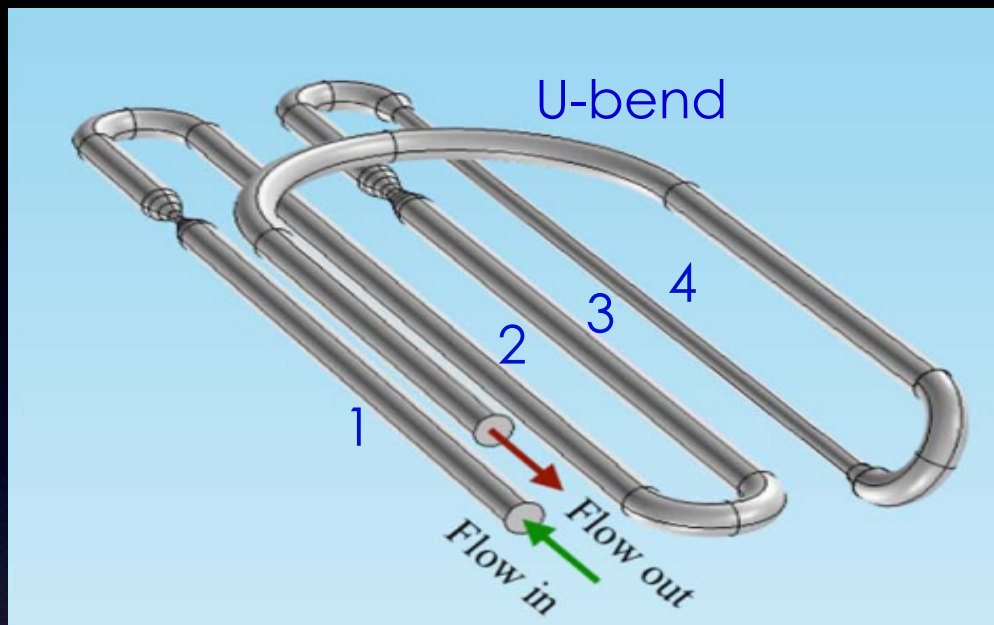
for known model parameters θ_m
and noise standard deviation σ .



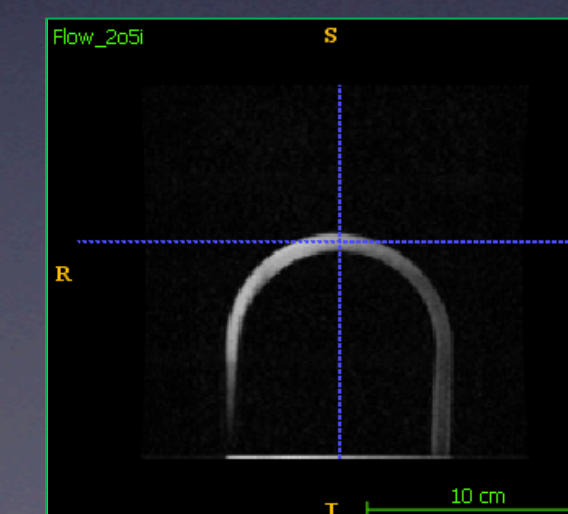
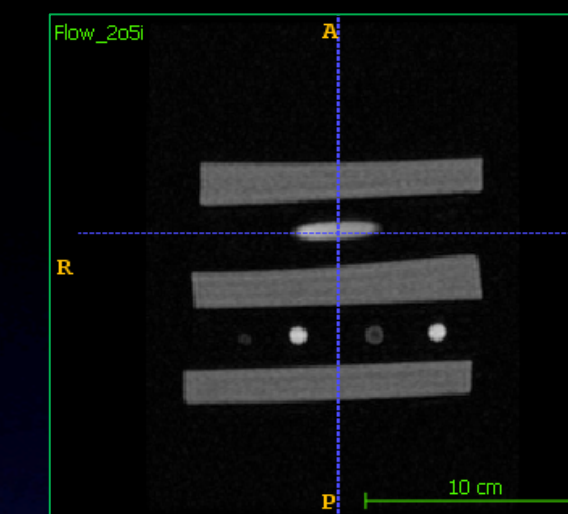
$N1, \dots, N6$ - channels count

Example 1

Blood-flow phantom 3D ToF MRI [14]

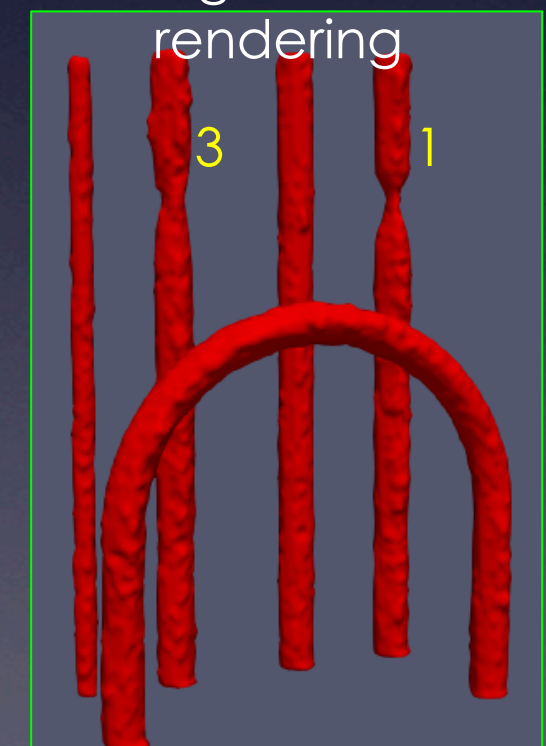


U-bend pipe inner radius: 4 mm



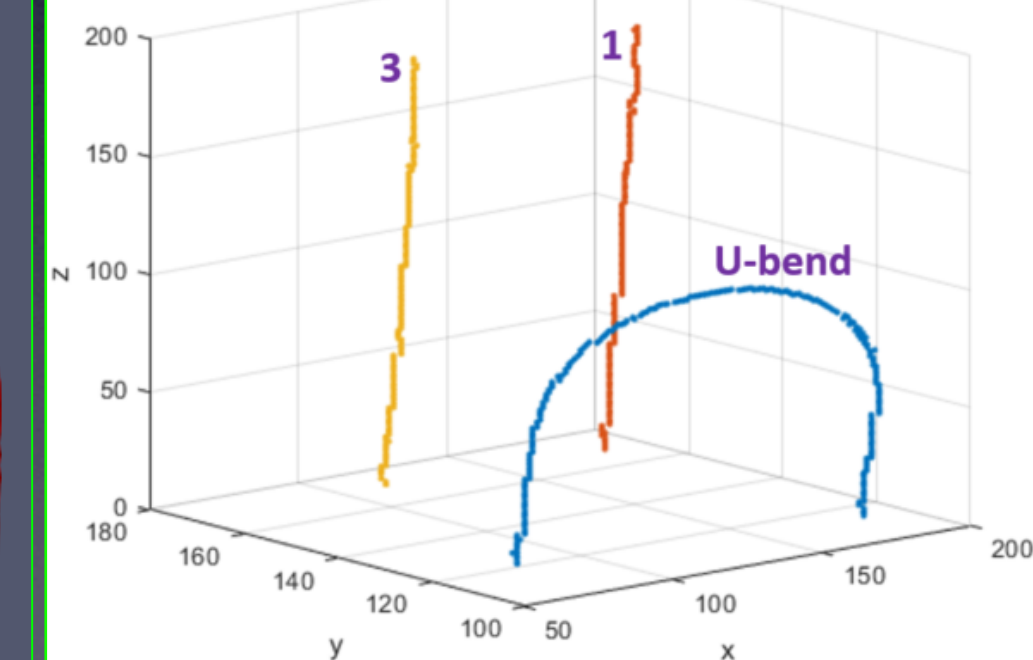
- MR-QA123 Quality Assurance Flow Phantom Set (Shelley)
- CardioFlow 1000 MR pump, 2.5 ml/s
- GE Signa HDxt 1.5 T scanner
- estimated *PSNR* = 30 dB
- voxels: 0.82mm x 0.82mm x 1.01mm

3D segmentation rendering



Binary skeletons

Flow_2o5i_v2-4_t15_Lx-sk.nii



Results [21]

Blood-flow phantom ToF MRA

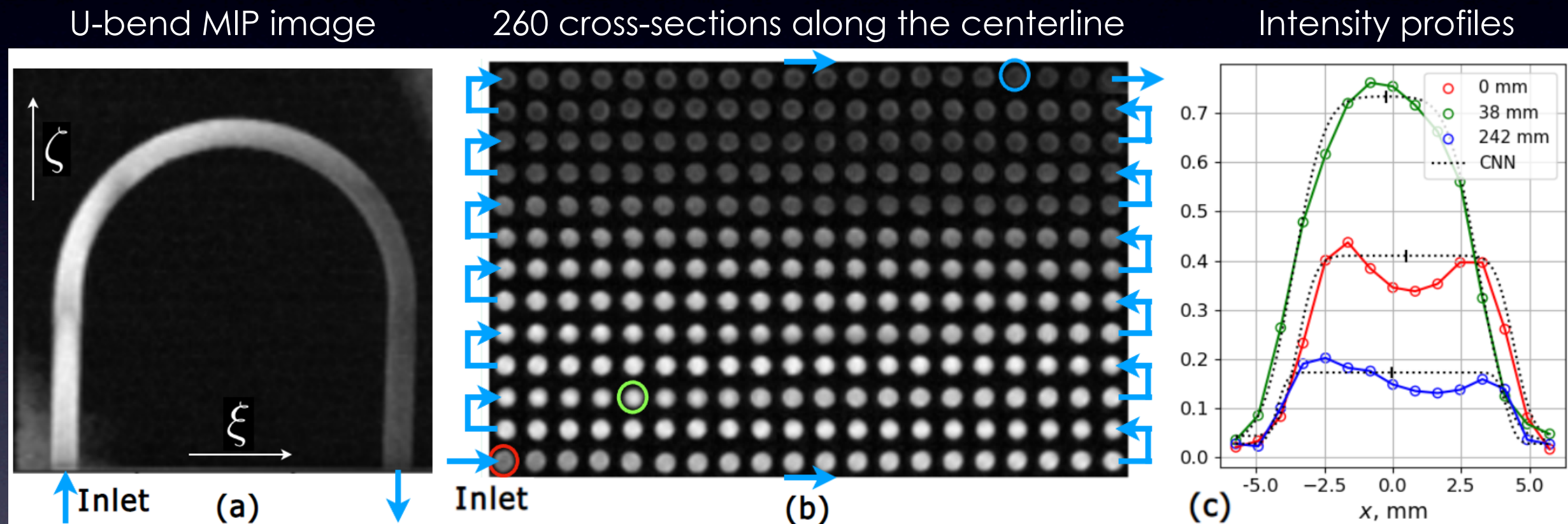
Image simulation
for transfer learning

$$\begin{aligned} 0 &\leq a \leq 0.3 \\ 0.1 &\leq b \leq 1.1 \\ 1 &\leq R/\Delta_s \leq 6 \\ 0.3 &\leq w/\Delta_s \leq 1.5 \\ -1.2 &\leq d_x/\Delta_s \leq 1.2 \\ -1.2 &\leq d_y/\Delta_s \leq 1.2 \\ \sigma &\approx 0.032 \end{aligned}$$

$M = 60\,000$ (training set)

$M_V = 20\,000$ (validation set)

$M_T = 20\,000$ (test set)



- Adam weight ϕ optimization
- ~1 hr of training up to the time of validation error increase, for a single-parameter output and (32,32,32,32,16,8) CNN channels

The sampling interval
 $\Delta_s = 0.82$ mm

Results [21]

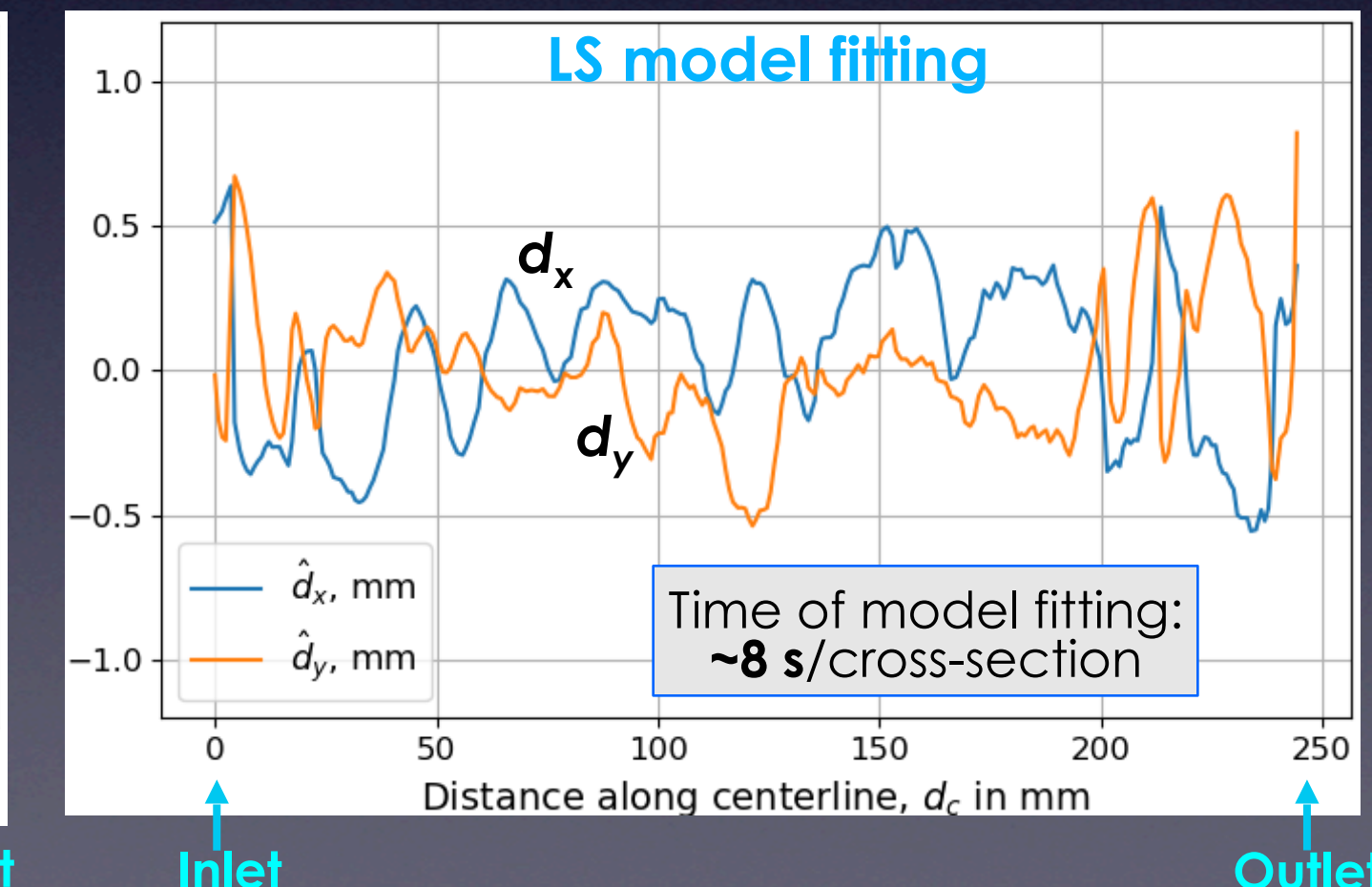
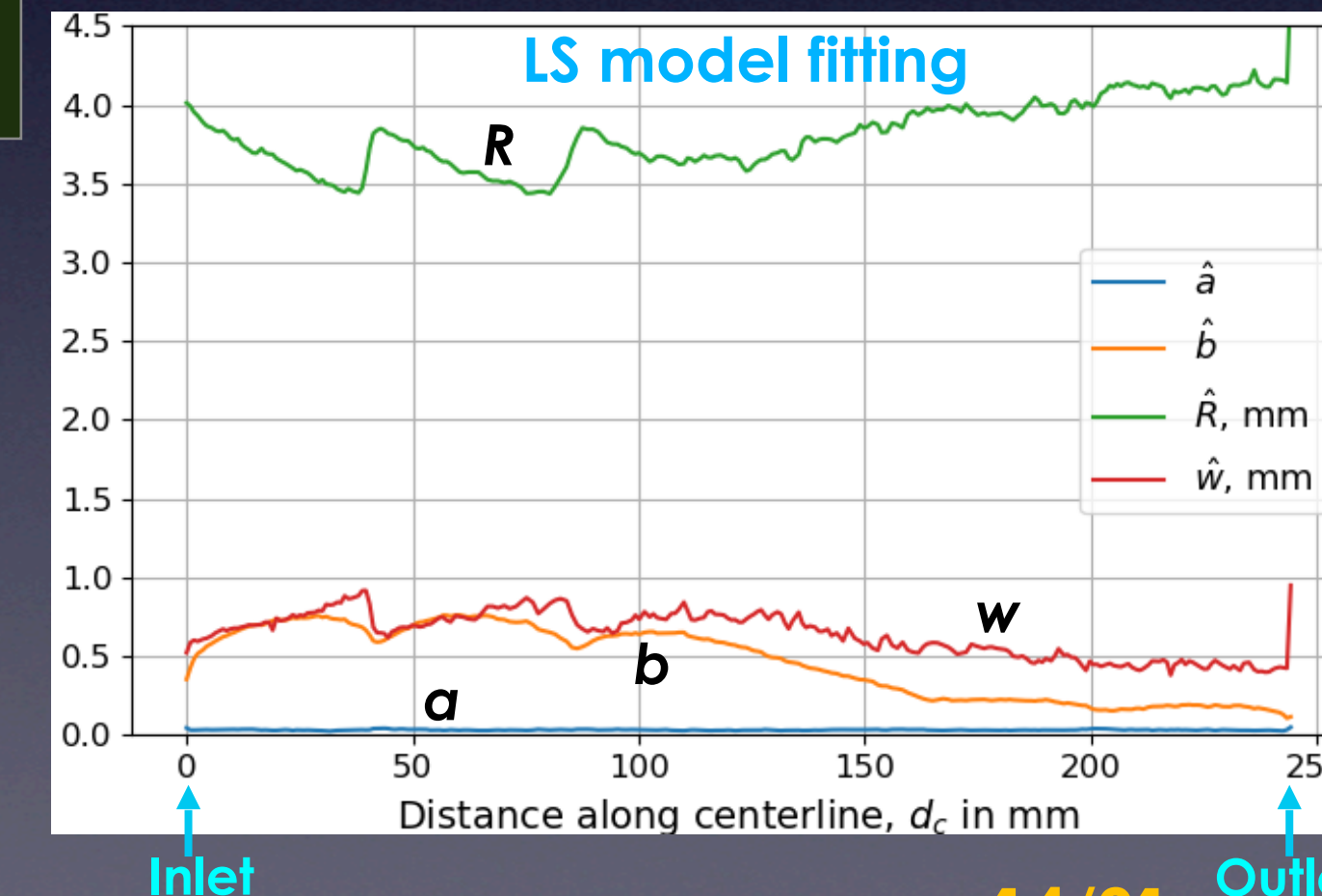
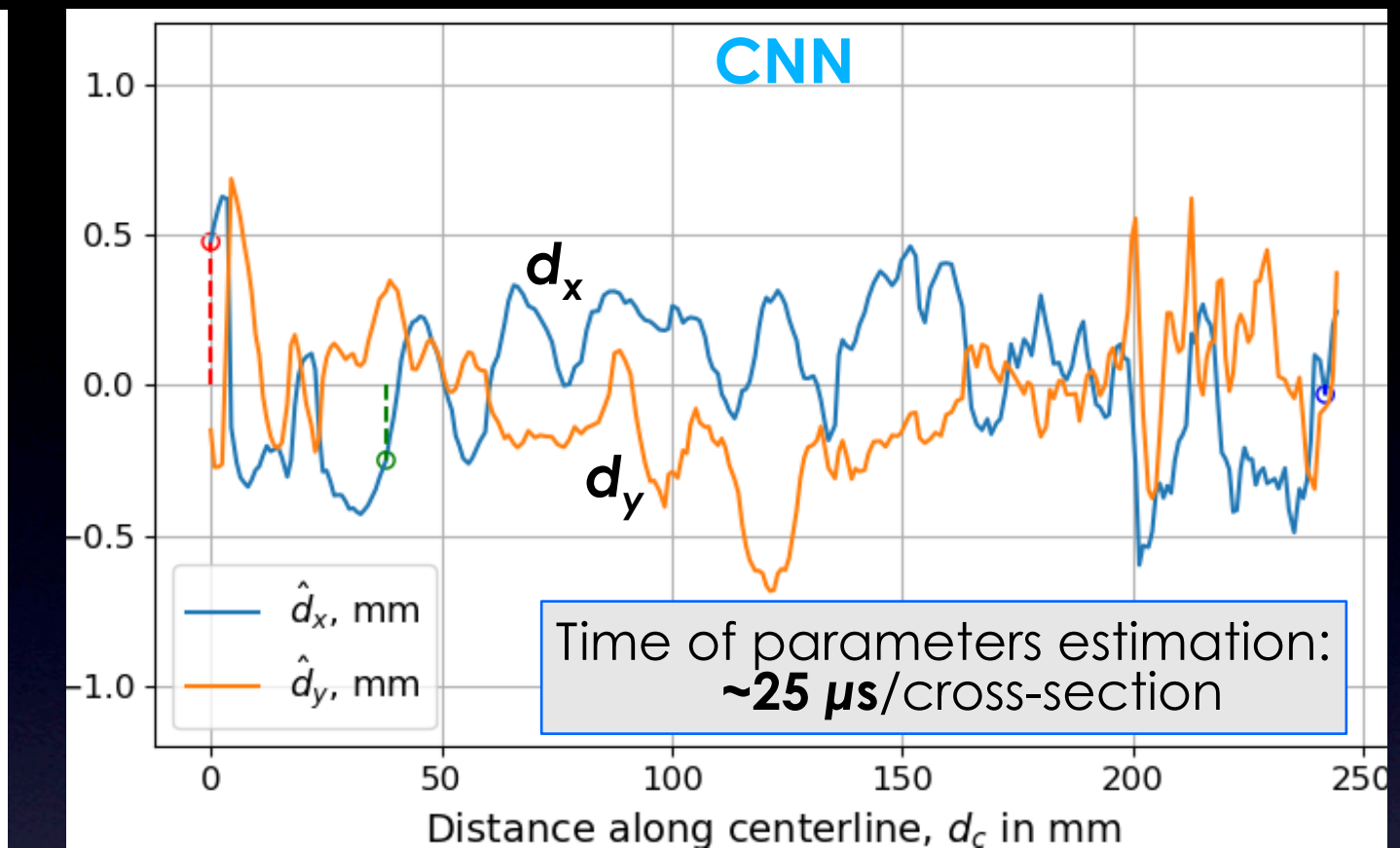
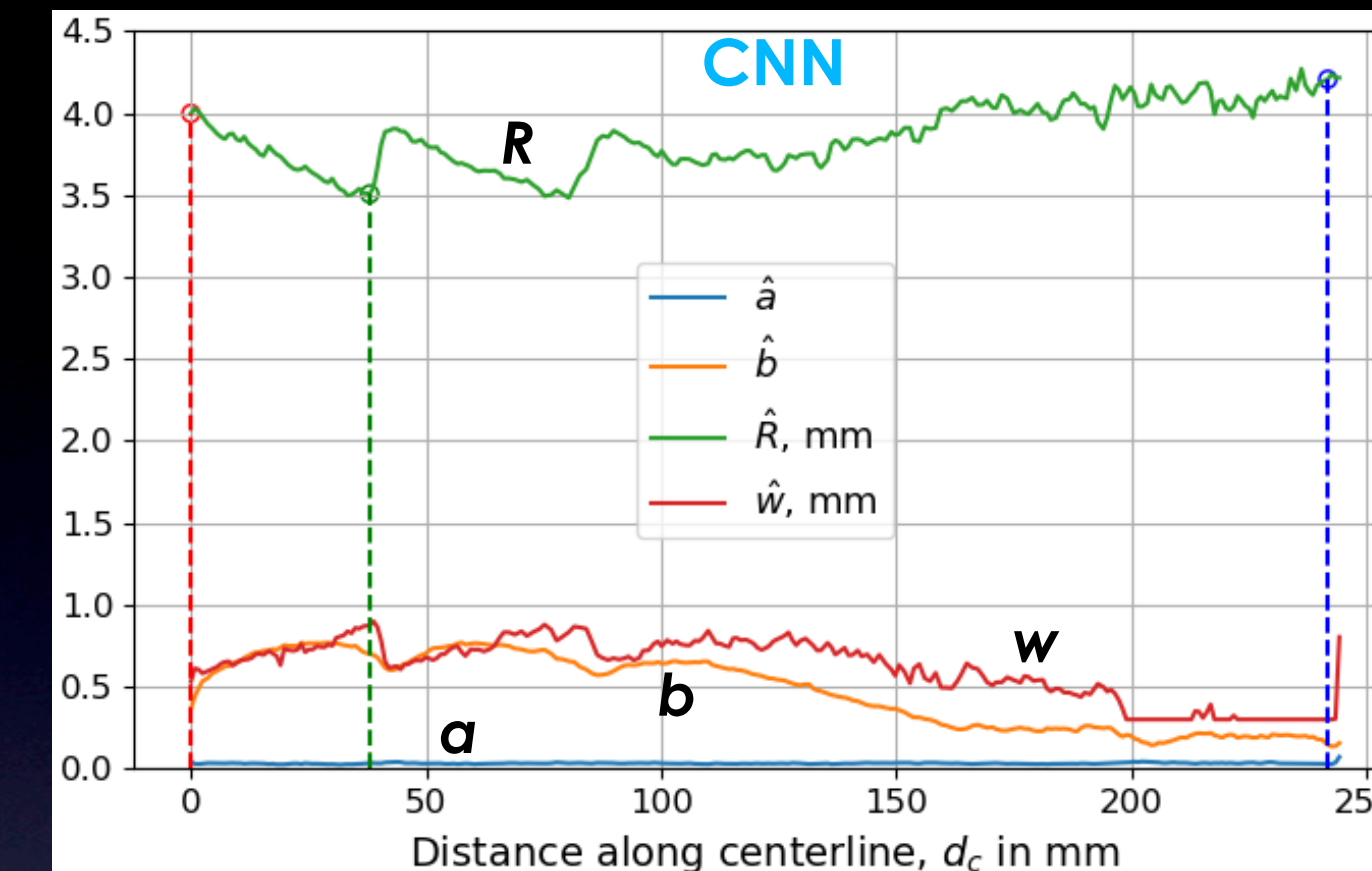
Blood-flow
phantom ToF MRA

Comparison

- Equally high accuracy
- CNN much faster

The sampling interval

$$\Delta_s = 0.82 \text{ mm}$$



Example 2

Coronary arteries in CE CTA [4,21]

- Rotterdam Coronary Artery Algorithms Evaluation Framework
- 17 datasets annotated by 3 observers
- voxels of different size: e.g. 0.3mm x 0.3mm x 0.4mm, 0.37mm x 0.37mm x 0.45mm, 0.43mm x 0.43mm x 0.25mm, ...

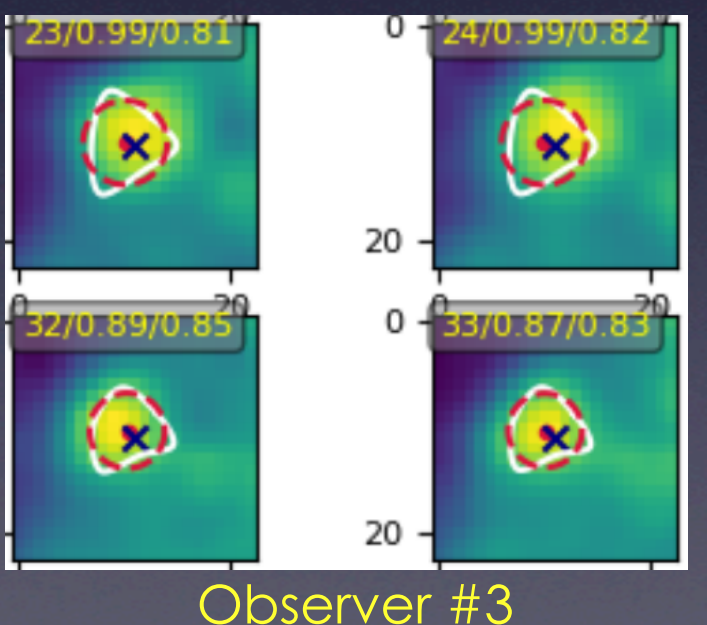
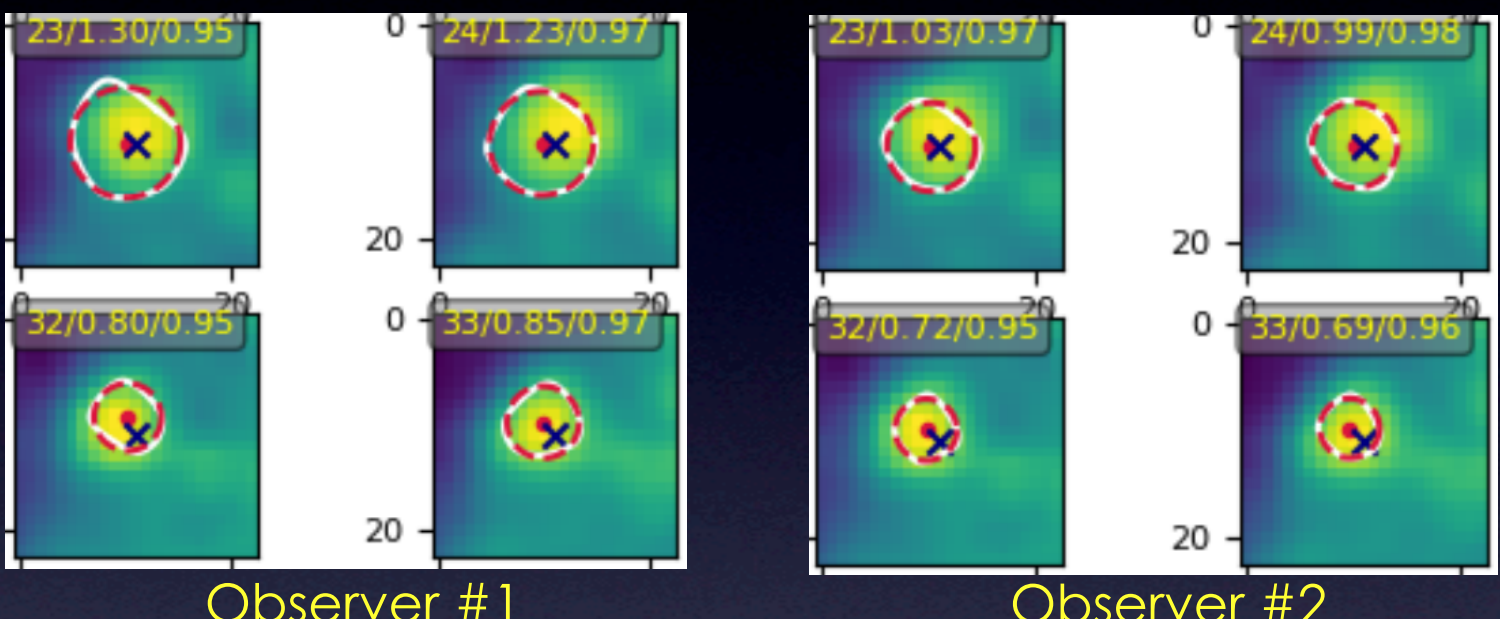
Black cross: centerline intersection point
 White line: contour marked by observer
 Red dot: center of mass of the contour
 Dashed red line: equivalent circle of radius

$$\rho = \sqrt{A/\pi} \quad (3)$$

where A is the area inside contour.

Values of (3) were substituted for radius R in (2).

LS model fitting --> errors and excessive computation time.



- The background intensity changes significantly across the image.
- The shape of marked contours differs much between the observers.

Results [21]

Equivalent radius of coronary arteries

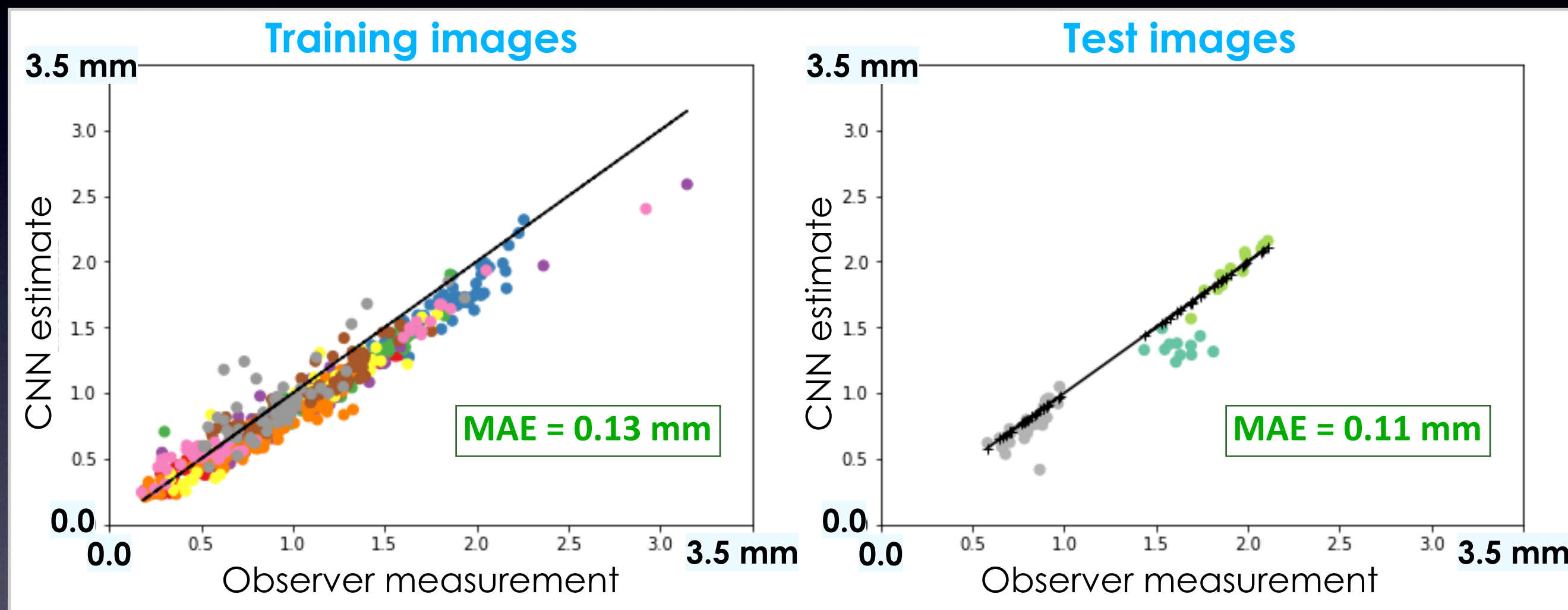
Training set: 558 sections of arteries segments annotated by Observer #1

Test set: 51 sections

The sampling interval
 $\Delta_s = 0.45 \text{ mm}$

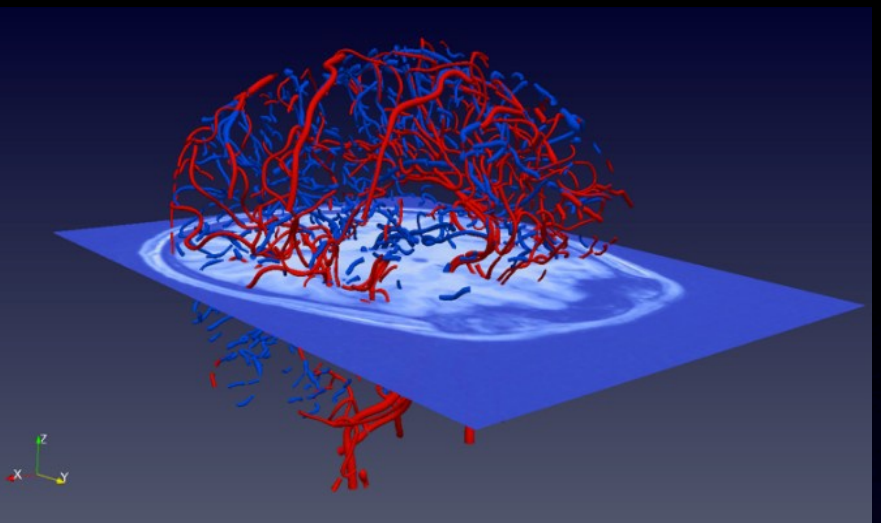
Center of mass shift estimation:
MAE < 0.09 mm
(another experiment, not shown here)

The CNN was trained on real, nonideal images to reduce the estimator sensitivity to spurious objects in the background.



Summary

1. Methods involving binary segmentation fail in performing the thin-branches extraction and quantification tasks.
2. Centerline-based image-formation-model fitting offers subvoxel accuracy, robustness to image nonidealities, and modularity for better processing control.
3. The CNN-based model parameters estimation is promising in terms of speed, accuracy, robustness and flexibility.



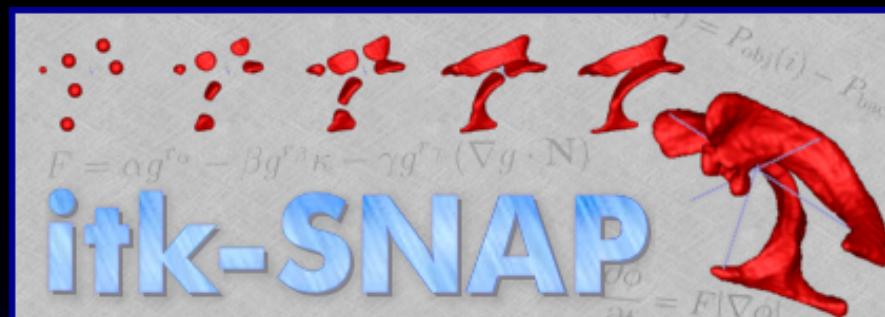
Future research

Automated 3D blood-vessel image processing methods, taking account of

- . vessel centerline tracking [11],
- . anatomical markers detection (e.g. ostia),
- . non-circular cross-sections (e.g. stenoses),
- . denoising,
- . superresolution [20].

Free software (visualization/segmentation/analysis)

.Multiplatform
.Interactive



itksnap.org/

University of Pennsylvania

Convert3D

MeshLab

meshlab.net

paraview.org/
ParaView

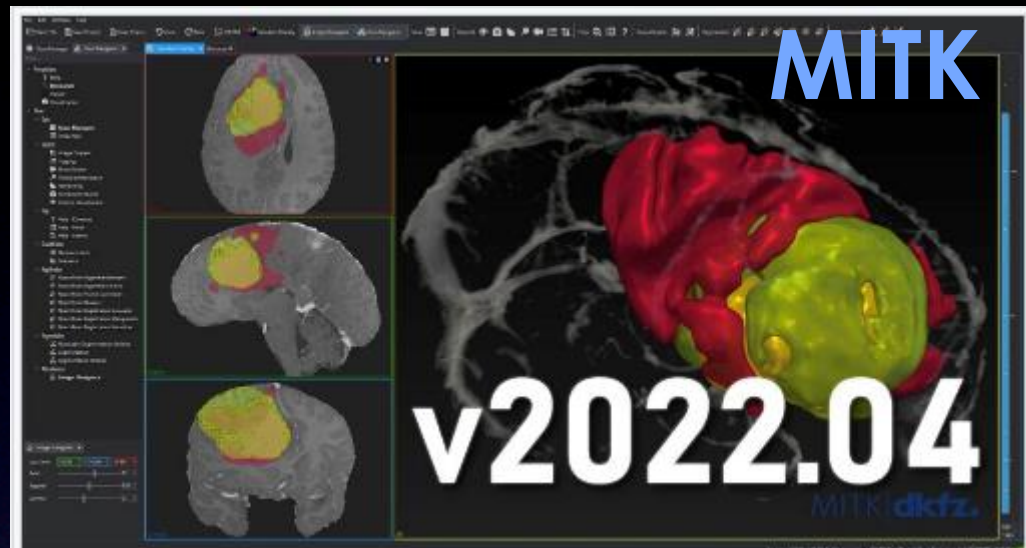
kitware | Glance

kitware.github.io/glance/



simvascular.github.io/

Harvard University
slicer.org/

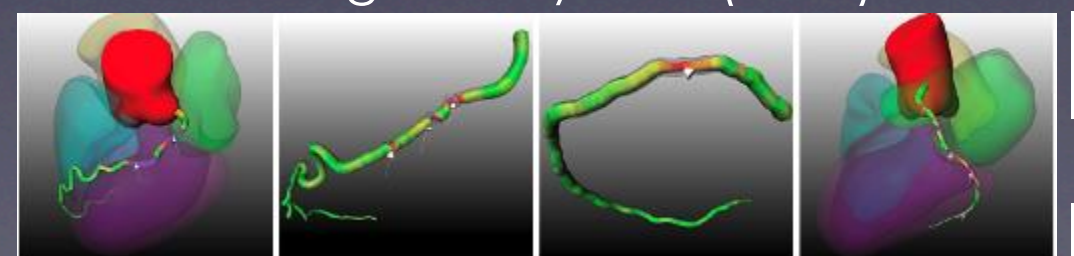


MITK
v2022.04

mitk.org/
German Cancer Research Center

Blood-vessel image datasets

Kirisli et al.: Standardized evaluation framework for evaluating coronary artery stenosis detection, stenosis quantification and lumen segmentation algorithms in computed tomography angiography, Medical Image Analysis 17 (2013) 859-876



PAVES

<https://paves.grand-challenge.org/>



NITRC
NeuroImaging Tools & Resources Collaboratory

<https://www.nitrc.org/projects/icbmra/>

Magnetic Resonance
Angiography Atlas Dataset

References

- [1] Methods involving binary segmentation fail in Tsao, C.W. et al.: Heart Disease and Stroke Statistics 2022 Update. *Circulation* 145, e153e639 (2022). doi: 10.1161/CIR.0000000000001052
- [2] Lesage, D., Angelini, D.E., Bloch I., Funka-Lea G.: A review of 3D vessel lumen segmentation techniques: models, features and extraction schemes. *Medical Image Analysis* 13, 819-845 (2009). doi: 10.1016/j.media.2009.07.011
- [3] Li, H., Tang, Z., Nan, Y., Yang, G.: Human tree-like tubular structure segmentation: A comprehensive review and future perspectives. *Computers in Biology and Medicine* 151, 106241 (2022). doi: 10.1016/j.combiomed.2022.106241
- [4] Schaap, M. et al.: Standardized evaluation methodology and reference database for evaluating coronary artery centerline extraction algorithms. *Medical Image Analysis* 13(5), 701714 (2009). doi: 10.1016/j.media.2009.06.003
- [5] Cheng, C.P.: Geometric Modeling of Vasculature. *Handbook of Vascular Motion*, 45-66, Academic Press (2019). doi: 10.1016/B978-0-12-815713-8.00004-8
- [6] Choi, G., Cheng, C.P., Wilson, N.M., Taylor, C.A.: Methods for Quantifying Three-Dimensional Deformation of Arteries due to Pulsatile and Nonpulsatile Forces: Implications for the Designs of Stents and Stent Grafts. *Annals of Biomedical Engineering* 37(1), 14-33 (2009). doi: 10.1007/s10439-008-9590-0
- [7] Sethian, J.A.: *Level Set Methods and Fast Marching Methods*. Cambridge University Press (2002)
- [8] Liu, Y., Kwak, H.S., Oh, I.S.: Cerebrovascular Segmentation Model Based on Spatial Attention-Guided 3D Inception U-Net with Multidirectional MIPs, *Applied Sciences*, 12, 2288, (2022). doi: 10.3390/app12052288
- [9] Materka, A. et al.: Automated modeling of tubular blood vessels in 3D MR angiography images. *IEEE 9th Int. Symp. On Image and Signal Processing and Analysis, ISPA 2015*, pp. 56-61. IEEE, Zagreb (2015). doi: 10.1109/ISPA.2015.7306032
- [10] Frangi, A.F., Niessen, W.J., Vincken, K.L., Viergever, M.A.: Multiscale Vessel Enhancement Filtering. In *Medical Image Computing and Computer-Assisted Intervention MICCAI98*, Wells, M. W., Colchester, A., and Delp, S. L. (Eds.), LNCS 1496, pp. 130-137 (1998). doi: 10.1007/BFb0056195

- [11] Wolterink, J.M., van Hamersveld, R.W, Viergever, M.A., Leiner, T., Igum, I.: Coronary artery centerline extraction in cardiac CT angiography using a CNN-based orientation classifier. *Medical Image Analysis* 51, 46-60 (2019). doi: 10.1016/j.media.2018.10.005
- [12] Chen, Z., Ning, R.: Three-dimensional point spread function measurement of cone-beam computed tomography system by iterative edge-blurring algorithm. *Physics in Medicine and Biology* 49, 1865-1880 (2004). doi: 10.1088/0031-9155/49/10/003
- [13] Materka, A., Mizushina, S.: Parametric signal restoration using artificial neural networks. *IEEE Transactions on Biomedical Engineering* 43(4), 357–372 (1996). doi: 10.1109/10.486256
- [14] Klepaczko, A., Szczypinski, P., Dwojakowski, G., Strzelecki, M., Materka, A.: Computer simulation of magnetic resonance angiography imaging: model description and validation, *PLOS ONE* 9(4), e93689 (2014). doi: 10.1371/journal.pone.0093689
- [15] Lamy, J., Merveille, O., Keerautret, B., Passat, N., Vacavant, A.: Vesselness Filters: A Survey with Benchmarks Applied to Liver Imaging, 2020 25th Int. Conf. On Pattern Recognition (ICPR), Milan, Italy, Jan 10-15, 2021.
- [16] Jerman, T., Pernus, F., Likar, B., Spiclin, Z.: Enhancement of Vascular Structures in 3D and 2D Angiographic Images, *IEEE Trans. On Medical Imaging* 35(9), 2016, 2107-2118.
- [17] Woerz, S.: 3D Model-Based Segmentation of 3D Biomedical Images. In *MEMICS 2014*, Hlineny et al. (Eds.), LNCS 8934, 40-46
- [18] Chen, Z. et al: Precise Measurement of Coronary Stenosis Diameter with CCTA Using CT Number Calibration, *Medical Physics* 46, Dec. 2019, 5514-5527
- [19] Hsu, C-Y. et al.: Gap-free segmentation of vascular networks with automatic image processing pipeline, *Computers in Biology and Medicine* 82, 2017, 29-39
- [20] Jurek, J., Kocinski, M., Materka, A., Elgalal, M., Majos, A.: CNN-based superresolution reconstruction of 3D MR images using thick-slice scans, *Biocybernetics and Biomedical Engineering* 40, 2019, 111-125
- [21] Materka, A., Jurek, J., Kocinski, M., Klepaczko, A.: CNN-Based Quantification of Blood Vessels Lumen in 3D Images. In J. Mikyška et al. (Eds.): *ICCS 2023*, LNCS 14074, pp. 1–9, 2023
- [22] Updegrove, A. et al.: SimVascular: An Open Source Pipeline for Cardiovascular Simulation, *Annals of Biomedical Engineering* 45, 2017, 525-541
- [23] Kollmannsberger, Kerschnitzki et al., "The small world of osteocytes: connectomics of the lacuno-canalicular network in bone." *New Journal of Physics* 19:073019, 2017.

Acknowledgment

The collaboration with

Dr. Artur Klepaczko
Dr. Marek Kociński
Prof. Michał Strzelecki
Prof. Piotr Szczypinski

Lodz University of Technology
Institute of Electronics

Dr. Marcin Elgalal
Prof. Agata Majos

Medical University of Lodz
Department of Radiology

Dr. Andreas Deistung
Prof. Jürgen R. Reichenbach

F. Schiller University in Jena
Medical Physics Group

Prof. Arvid Lundervold
Prof. Carlos Vinhais

University of Bergen
Department of Biomedicine
Polytechnic Institute of Porto
ISEP School of Engineering

is much appreciated.

Parts of this work were supported by Polish National Science Center
under Grant No. 2013/08/M/ST7/00943.